Spectroscopic Studies of the Active Site of Galactose Oxidase

Peter F. Knowles,[†] Rodney D. Brown III,[‡] Seymour H. Koenig,[‡] Shengke Wang,[§] Robert A. Scott,[§] Michele A. McGuirl,[⊥] Doreen E. Brown,[⊥] and David M. Dooley*,[⊥]

Department of Biochemistry and Molecular Biology, University of Leeds, Leeds, LS2 9JT, U.K., IBM Thomas J. Watson Research Center, Yorktown Heights, New York 10598, Center for Metalloenzyme Studies, University of Georgia, Athens, Georgia 30602, and Department of Chemistry and Biochemistry, Montana State University, Bozeman, Montana 59717

Received August 24, 1994[⊗]

X-ray absorption and EPR spectroscopy have been used to probe the copper site structure in galactose oxidase at pH 4.5 and 7.0. The results suggest that there are no major differences in the structure of the tetragonal Cu(II) site at these pH values. Analysis of the extended X-ray absorption fine structure (EXAFS) indicates that four N,O scatterers are present at approximately 2 Å; these are presumably the equatorial ligands. In addition, the EXAFS data establish that oxidative activation to produce the active-site tyrosine radical does not cause major changes in the copper coordination environment. Therefore results obtained on the one-electron reduced enzyme, containing Cu(II) but not the tyrosine radical, probably also apply to the catalytically active Cu(II)/tyrosine radical state. Solvent water exchange, inhibitor binding, and substrate binding have been probed via nuclear magnetic relaxation dispersion (NMRD) measurements. The NMRD profile of galactose oxidase is quantitatively consistent with the rapid exchange of a single, equatorial water ligand with a Cu(II)−O separation of about 2.4 Å. Azide and cyanide displace this coordinated water. The binding of azide and the substrate dihydroxyacetone produce very similar effects on the NMRD profile of galactose oxidase, indicating that substrates also bind to the active site Cu(II) in an equatorial position.

Introduction

Galactose oxidase catalyzes the two-electron oxidation of an alcohol carbon to an aldehyde, as illustrated in eq 1. A wide

$$RCH_2OH + O_2 \rightarrow RCHO + H_2O_2 \qquad (1)$$

variety of hexoses, hexose derivatives, and other primary alcohols are oxidized with strict stereospecificity.[1] For example, D-galactose is the best substrate among hexoses but L-galactose is not oxidized at all. Galactose oxidase is a monomer (M_r = 68 kD) composed of three domains and containing a single copper ion essential for catalytic activity.[1−3] The structure of galactose oxidase was recently solved at 1.7-Å resolution;[4,5] the active site region, including the copper coordination geometry, is shown in Figure 1. No other prosthetic groups or cofactors are evident in the high-resolution structure. The copper is located on the solvent-accessible surface of the second domain forming the bottom of a well and surrounded by hydrophobic and aromatic residues. In acetate buffer at pH 4.5 the Cu(II) has square-pyramidal coordination (Figure 1) with the phenolate O of Tyr272, the N_ϵ atoms of His496 and His581, and the acetate forming a nearly perfect plane. Tyr495 is coordinated axially at a relatively long distance of 2.7 Å, compared to an average of about 2.1 Å for the equatorial ligands (Figure 1). Square-pyramidal coordination with tyrosine, histidine, and at least one solvent-derived ligand had been predicted from a variety of spectroscopic studies.[1−3,6−10] The observation that the activity of galactose oxidase is much lower at pH 4.5 than at pH 7.0[11] may be related to buffer coordination.

A mononuclear copper site, together with the absence of any other cofactors, raised the interesting question of how the enzyme catalyzes two-electron redox chemistry, since copper normally functions as a one-electron redox unit. This issue, and the observation that galactose oxidase can be *oxidatively* activated, led Hamilton to propose the involvement of a Cu(III) ⇌ Cu(I) redox couple in turnover.[11] Over the past few years elegant work by the Whittakers has established that the second redox cofactor in galactose oxidase is a tyrosine radical.[6,12−14] Oxidative activation of the enzyme by mild oxidants produces a Cu(II)−tyr$^\bullet$ state, which is EPR silent owing to strong antiferromagnetic coupling between the d^9 Cu(II) and the unpaired electron of the tyrosine radical.[6] As normally isolated, the resting enzyme is a mixture of varying proportions of the Cu(II)−tyr$^\bullet$ state and a reduced, inactive form with Cu(II)−tyr,[7] which do not rapidly interconvert in the absence of

* To whom correspondence should be addressed.
[†] University of Leeds.
[‡] IBM (now at Relaxometry, Inc., Mahopac, NY 10541).
[§] University of Georgia.
[⊥] Montana State University.
[⊗] Abstract published in *Advance ACS Abstracts,* June 15, 1995.

(1) Knowles, P. F.; Ito, N. In *Perspectives in Bio-inorganic Chemistry*; Jai Press LTD: London, 1994; Vol. 2, pp 207−244.
(2) Ettinger, M. J.; Kosman, D. J. In *Copper Proteins*; Spiro, T. G., Ed.; Wiley: New York, 1981; pp 220−261.
(3) Kosman, D. J. In *Copper Proteins and Copper Enzymes*; Lontie, R., Ed.; CRC Press: Boca Raton, FL, 1984; Vol. II; pp 1−26.
(4) Ito, N.; Phillips, S. E. V.; Stevens, C.; Ogel, Z. B.; McPherson, M. J.; Keen, J. N.; Yadav, K. D. S.; Knowles, P. F. *Nature* **1991**, *350*, 87−90.
(5) Ito, N.; Phillips, S. E. V.; Yadav, K. D. S.; Knowles, P. F. *J. Mol. Biol.* **1994**, *238*, 794−814.
(6) Whittaker, J. W. In *Bioinorganic Chemistry of Copper*; Karlin, K. D., Tyeklar, Z., Eds.; Chapman and Hall: New York, 1993; pp 447−458.
(7) Whittaker, M. M.; Whittaker, J. W. *J. Biol. Chem.* **1988**, *263*, 6074−6080.
(8) Kosman, D. J.; Peisach, J.; Mims, W. B. *Biochemistry* **1980**, *19*, 1304−1308.
(9) Marwedel, B. J.; Kosman, D. J.; Bereman, R. D.; Kurland, R. J. *J. Am. Chem. Soc.* **1981**, *103*, 2842−2847.
(10) Giordano, R. S.; Bereman, R. D.; Kosman, D. J.; Ettinger, M. J. *J. Am. Chem. Soc.* **1974**, *196*, 1023−1026.
(11) Hamilton, G. A.; Adolf, P. K.; de Jersey, J.; DuBois, G. C.; Dyrkacz, G. R.; Libby, R. D. *J. Am. Chem. Soc.* **1978**, *100*, 1899−1912.
(12) Whittaker, M. M.; DeVito, V. L.; Asher, S. A.; Whittaker, J. W. *J. Biol. Chem.* **1989**, *264*, 7104−7106.
(13) Whittaker, M. M.; Whittaker, J. W. *J. Biol. Chem.* **1990**, *265*, 9610−9613.
(14) Babcock, G. T.; El-Deeb, M. K.; Sandusky, P. O.; Whittaker, M. M.; Whittaker, J. W. *J. Am. Chem. Soc.* **1992**, *114*, 3727−3734.

0020-1669/95/1334-3895$09.00/0

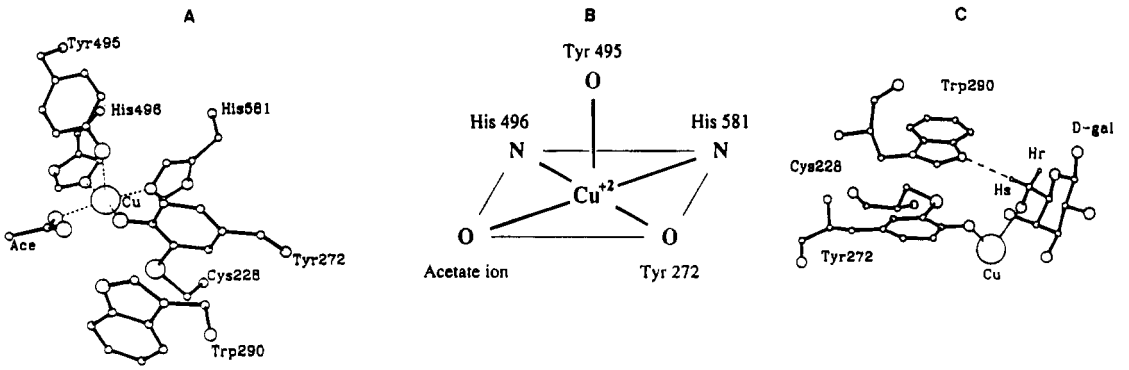

Figure 1. Views of the galactose oxidase active site. (A) Structure of the copper site at pH 4.5 showing the protein ligands and the coordinated acetate. (B) Schematic illustration of the copper coordination geometry. (C) Plausible model for the binding of (D)-galactose to the galactose oxidase active site. This model is based on "docking" a molecule of (D)-galactose into the crystallographic structure of resting galactose oxidase at pH 7.0.

exogenous oxidants or reductants. X-ray absorption spectroscopy showed that substrate alcohols reduce the active site redox couple by two electron equiv giving a Cu(I)−tyr state.[15] Examination of the active-site structure determined by X-ray diffraction revealed a novel covalent thioether bond between Tyr272 and Cys228 (Figure 1). The cysteine sulfur and β-carbon are coplanar with the Tyr272 ring.[4,5] EPR and ENDOR spectra are fully consistent with *ortho*-substitution of the tyrosine radical.[13,14] Another intriguing feature of the active-site structure is the stacking of Trp290 with Tyr272 and the thioether group; the distance between the planes of these groups is only 3.4 Å.[4,5] The novel thioether bond and the stacking with Trp290 may serve to stabilize the tyrosine radical. Amino acid radicals have now been identified or implicated in several enzymes.[16,17]

Despite the rapid progress toward achieving a detailed understanding of the structure and mechanism of galactose oxidase, many fundamental questions have not yet been addressed. For example, uncertainty remains concerning the form of the enzyme that has been crystallographically characterized; i.e. Cu(II)−tyr•, or Cu(II)−tyr, or a mixture. Spectroscopic comparisons among the different forms are therefore a valuable way to assess active-site structural variations. Another question is the possibility of a significant change in the Cu(II) coordination geometry between pH 4.5 and 7.0. When a galactose oxidase crystal is transferred to a pH 7.0 buffer lacking acetate, the coordinated acetate is lost. At pH 7.0 a water molecule appears to be present near the original location of the acetate but at a Cu(II)−O coordination distance of 2.8 Å.[5] Since this distance is probably too long to represent a substantial Cu(II)−OH_2 bond, the crystallographic study suggests that the copper geometry is effectively distorted-pyramidal and approximately three-coordinate. None of the previous spectroscopic experiments appear to be consistent with such a geometry at pH 7.0. Additional experiments are required to reconcile the current results. Finally, Ito *et al.* have presented a model for substrate binding to copper (Figure 1C) that straightforwardly rationalizes the observed substrate specificity. Direct crystallographic evidence in favor of this model is lacking, however, since crystal packing factors block access to the active site by substrates.[5] Consequently, solution spectroscopic studies are perhaps the best approach to examine substrate binding at this time.

We have initiated a series of spectroscopic experiments to address these issues. X-ray absorption spectroscopy (XAS) has become an extremely informative probe of the coordination environment of metal sites in proteins.[18,19] XAS (both in the edge and EXAFS regions) and EPR are very effective methods for detecting and defining structural perturbations of copper sites. Solvent proton nuclear magnetic relaxation dispersion (NMRD) measurements are an excellent means to probe exogenous ligand binding to copper−protein active sites where solvent is coordinated to a paramagnetic Cu(II) center.[20,21] Here we report the results of XAS, EPR, and NMRD studies on the galactose oxidase active site.

Experimental Section

Galactose oxidase was purified as previously described[5,22] and displayed activity and electrophoretic behavior identical to the preparations used for the crystallographic experiments. Oxidatively activated galactose oxidase and reduced (inactive) galactose oxidase, corresponding to the Cu(II)−tyr• and Cu(II)−tyr forms, respectively, were prepared as previously described,[7] except that K_3IrCl_6 was used as the oxidant. Only a slight stoichiometric excess of K_3IrCl_6 was used, and it was removed by gel filtration within minutes of addition. The activity of oxidized galactose oxidase is the same whether hexachloroiridate or ferricyanide is used. Metal-depleted galactose oxidase was prepared by overnight dialysis against 20 mM sodium diethyldithiocarbamate in 20 mM PIPES buffer, pH 7.0. The sample was centrifuged and dialyzed against the PIPES buffer containing 1 mM EDTA and then against Chelexed PIPES buffer. XAS samples were generally prepared in the following manner. Adventitious metals were removed by extensive dialysis of dilute protein samples (2−10 mg/mL) against Chelexed 0.1 M sodium phosphate buffer, pH 7.0. In order to increase the protein solubility, a sufficient volume of 8 M urea, previously purified by passage through a Dowex MR3 column, was then added to each sample to give a final urea concentration of 2 M. Galactose oxidase activity is reported to be *not affected* by moderate concentrations of urea,[23] and this was confirmed. Samples were immediately concentrated in a MicroProDiCon apparatus (Spectrum) to approximately 1 mM. Some samples were prepared by similar methods in 20 mM PIPES (pH 7.0) or 0.25 M sodium acetate buffer (pH 4.5) for direct comparison of the copper EXAFS and edges at these pH values. Copper X-ray absorption edge and EXAFS data were collected at the Stanford Synchrotron Radiation Laboratory and the National Synchrotron Light Source at Brookhaven National Laboratory. Data reduction was carried out using the XFPAK software developed by one of us

(15) Clark, K.; Penner-Hahn, J. E.; Whittaker, M. M.; Whittaker, J. W. *J. Am. Chem. Soc.* **1990**, *112*, 6433−6434.
(16) Stubbe, J. *Biochemistry* **1988**, *27*, 3893−3900.
(17) Pedersen, J. Z.; Finazzi-Agró, A. *FEBS Lett.* **1993**, *325*, 53−58.
(18) Doniach, S.; Eisenberger, P.; Hodgson, K. O. In *Synchrotron Radiation Research*; Winick, H., Doniach, S., Eds.; Plenum: New York, 1980; pp 425−428.
(19) Scott, R. A. *Methods Enzymol.* **1985**, *117*, 414−459.
(20) Dooley, D. M.; McGuirl, M. A.; Cote, C. E.; Knowles, P. F.; Singh, I.; Spiller, M.; Brown, R. D. III; Koenig, S. H. *J. Am. Chem. Soc.* **1991**, *113*, 754−761.
(21) Bertini, I.; Luchinat, C. *NMR of Paramagnetic Molecules in Biological Systems*; Benjamin/Cummings: Menlo Park, CA, 1986.
(22) Tressel, P.; Kosman, D. J. *Anal. Biochem.* **1980**, *105*, 150−153.
(23) Kosman, D. J.; Ettinger, M. J.; Weiner, R. E.; Massaro, E. J. *Arch. Biochem. Biophys.* **1974**, *165*, 456−467.

Table 1. X-ray Absorption Spectroscopic Data Collection and Reduction for Galactose Oxidase Samples

	edges	EXAFS (A/B)[a]
SR facility	SSRL	NSLS/SSRL
beamline	VII-3	X10C/VII-3
monochromator crystal	Si[220]	Si[111]/Si[220]
detection method	fluorescence	fluorescence
detector type	13-element solid state array[b]	13-element solid state array[c/b]
scan length, min	15	30/21
scans in average	2	12/15
metal concn, mM	0.8−2.0	0.8−2.0
temp, K	10	12/10
energy standard	Cu foil (1st inflection)	Cu foil (1st inflection)
energy calibration, eV	8980.3	8980.3
E_0, eV	9000	9000
pre-edge bckgd energy range, eV (polynomial order)	9050−9380(2)[d]	9050−9650(2)[d]
spline bckgd energy range, eV (polynomial order)	9200−9380(2)	9030−9200(2) 9200−9400(3) 9400−9650(3)

[a] The XAS data for the $Fe(CN)_6^{4-}$-reduced galactose oxidase sample are the average of data collected at NSLS (A) and SSRL (B). Where data collection parameters were different from data sets A and B, values are separated by /. Data for other samples were collected at SSRL using the parameters specified for data set B. [b] Maintained by NIH Biotechnology Research Resource at SSRL. [c] Courtesy of G. N. George, now at SSRL. [d] Background was calculated from fitting this (EXAFS) rigion; then a constant subtracted so that the background matched the data just before the edge.

(R.A.S.), as described previously.[19] Details of the data collection and reduction are summarized in Table 1. Curve-fitting analyses of the EXAFS data were performed using EXCURV86, which makes use of curved-wave single- and multiple-scattering.[24] All scattering functions were calculated within EXCURV86 and verified using model compound EXAFS data. First-shell scattering functions were checked against model compound-tested FEFF v3.25[25] scattering function "templates" as described previously,[26] yielding $\Delta E_0 = 32.0$ eV, this value being fixed in all subsequent curve-fitting of galactose oxidase data. The amplitude reduction factor was also fixed at a value of 0.9 for all fits. A constrained group refinement procedure was used in fitting histidyl imidazoles.[27] Curve-fitting procedures are fully described in ref 27.

NMRD measurements of the longitudinal relaxation rate ($1/T_1$) of solvent protons and data analysis were carried out along the lines described earlier using the relaxometer at IBM.[20] NMRD changes induced by azide binding were analyzed by a standard Scatchard analysis.[28] Because the binding constant for DHA binding is much smaller than that for azide, the saturation point could not be reached in the DHA titration and a Scatchard analysis was therefore unreliable. Instead the data were analyzed by transforming eq 2 and solving for y_i, as expressed in eq 3. A_i is the free ligand concentration; b_i is the

$$b_i/C = A_i/(K + A_i) \quad (2)$$

$$y_i = {}^1/_2\{2k - a(C + K + L_i) + [(2k - a[C + K + L_i])^2 - 4a(L_i[aC - k] - k[C + K])]^{1/2}\} \quad (3)$$

concentration of bound ligand L; L_i is the total ligand concentration ($A_i + b_i = L_i$); C is the total concentration of enzyme; y_i is the measured relaxation rate at a given L_i and frequency; K is the equilibrium (binding) constant; k is the value of the relaxation rate at [azide] = 0 at each frequency. The value of the relaxation rate (y_i) at $A_i = \infty$ is defined as $k - aC$, where a is an adjustable parameter.[29] A best fit to this function was performed using RS/1 (Release 4.4.1, BBN Inc.). A Bruker 220D-SRC instrument was used for the EPR experiments. Data were collected and manipulated using programs from Scientific Software Services running on an IBM PS/2. Additional details may be found in the figure legends.

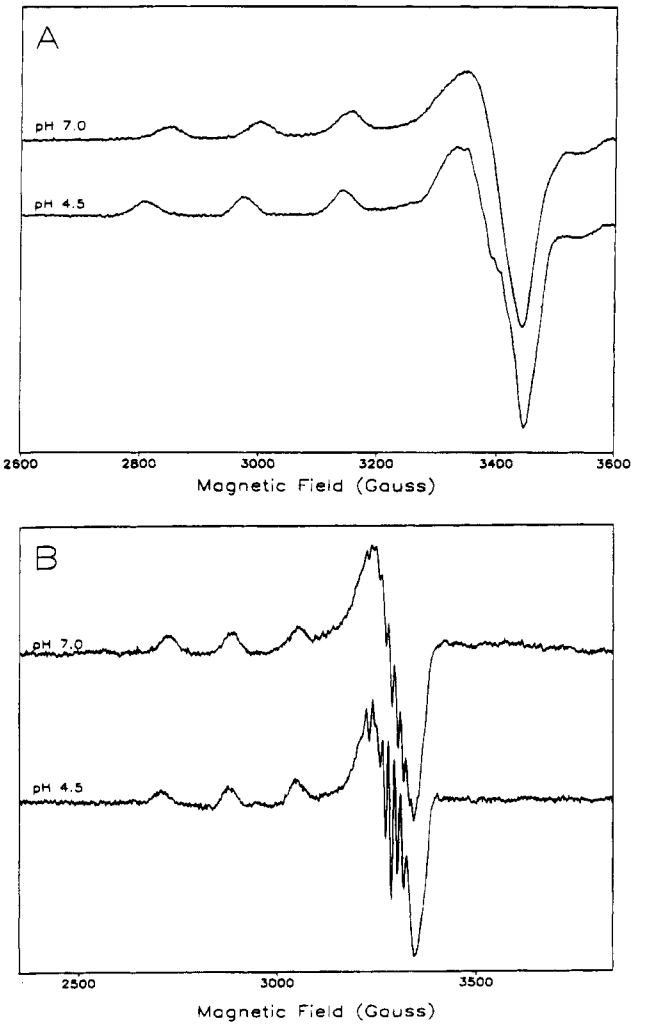

Figure 2. EPR spectra of ferrocyanide-reduced galactose oxidase at pH 4.5 and 7.0. (A) Room-temperature spectra at 9.80 GHz in a rectangular glass microslide, with a modulation amplitude of 20 G. Parameters estimated from these spectra are as follows. pH 7.0: $g_{\|} = 2.280$; $g_{\perp} = 2.069$; $A_{\|} = 175 \times 10^{-4}$ cm^{-1}; pH 4.5: $g_{\|} = 2.282$; $g_{\perp} = 2.064$; $A_{\|} = 183 \times 10^{-4}$ cm^{-1} (B) 77 K spectra at 9.48 GHz with a modulation amplitude of 3.2 G. Parameters estimated from these spectra are as follows. pH 7.0: $g_{\|} = 2.294$; $g_{\perp} = 2.062$; $A_{\|} = 176 \times 10^{-4}$ cm^{-1}; $A_N = 13.4 \times 10^{-4}$ cm^{-1}. pH 4.5: $g_{\|} = 2.284$; $g_{\perp} = 2.068$; $A_{\|} = 181 \times 10^{-4}$ cm^{-1}; $A_N = 12.9 \times 10^{-4}$ cm^{-1}.

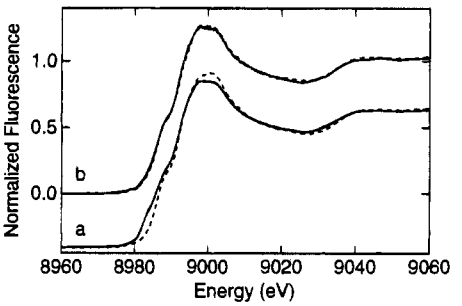

Figure 3. Copper K-edge X-ray absorption spectra of galactose oxidase. (A) Edges for the ferrocyanide-reduced (—) and ferricyanide-oxidized (- - -) forms. (B) Edges for resting galactose oxidase at pH 4.5 (- - -) and 7.0 (—).

Results and Discussion

Assessment of Active-Site Structure. Few spectroscopic studies have been conducted under the conditions used to obtain

(24) Strange, R. W.; Blackburn, N. J.; Knowles, P. F.; Hasnain, S. S. *J. Am. Chem. Soc.* **1987**, *109*, 7157−7162.
(25) Rehr, J. J.; Leon, J. M.; Zabinsky, S. I.; Albers, R. C. *J. Am. Chem. Soc.* **1991**, *113*, 5135−5140.

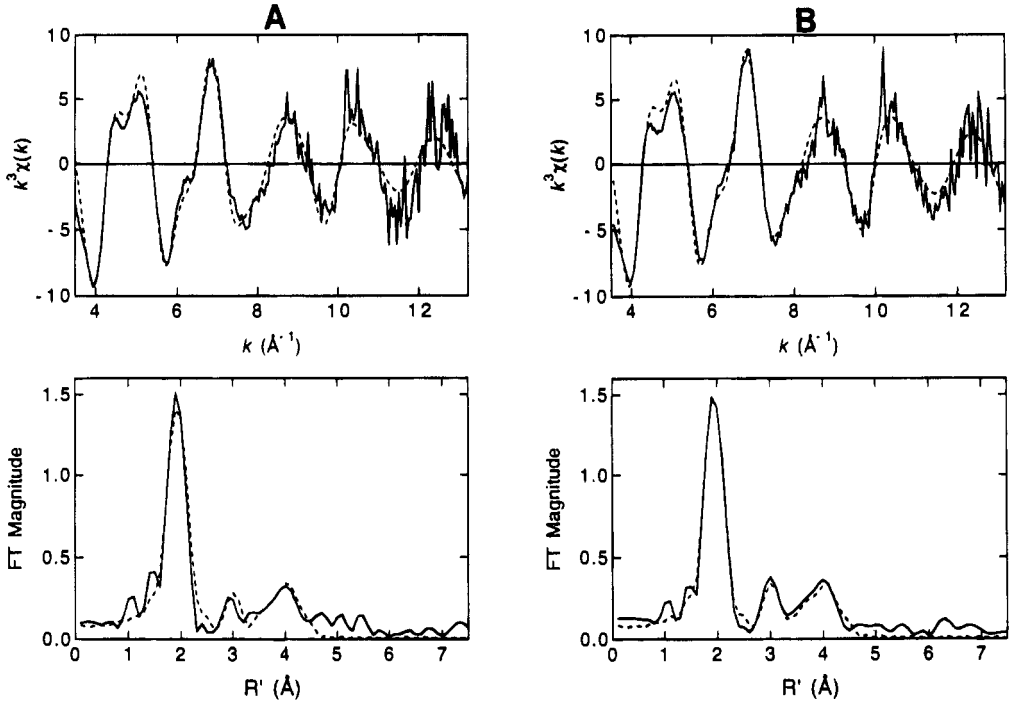

Figure 4. Galactose oxidase EXAFS (top) and Fourier transforms (bottom) at pH 7.0 and 4.5. (A) Resting (as isolated) galactose oxidase at pH 7.0. (B) Resting (as isolated) galactose oxidase at pH 4.5. For data in this figure and Figure 5, FTs were computed over the range $k = 3.5-13.5$ Å^{-1}, were k^3-weighted, and were phase corrected using Cu–N phase shifts. The fits from Table 2 are shown as dashed lines.

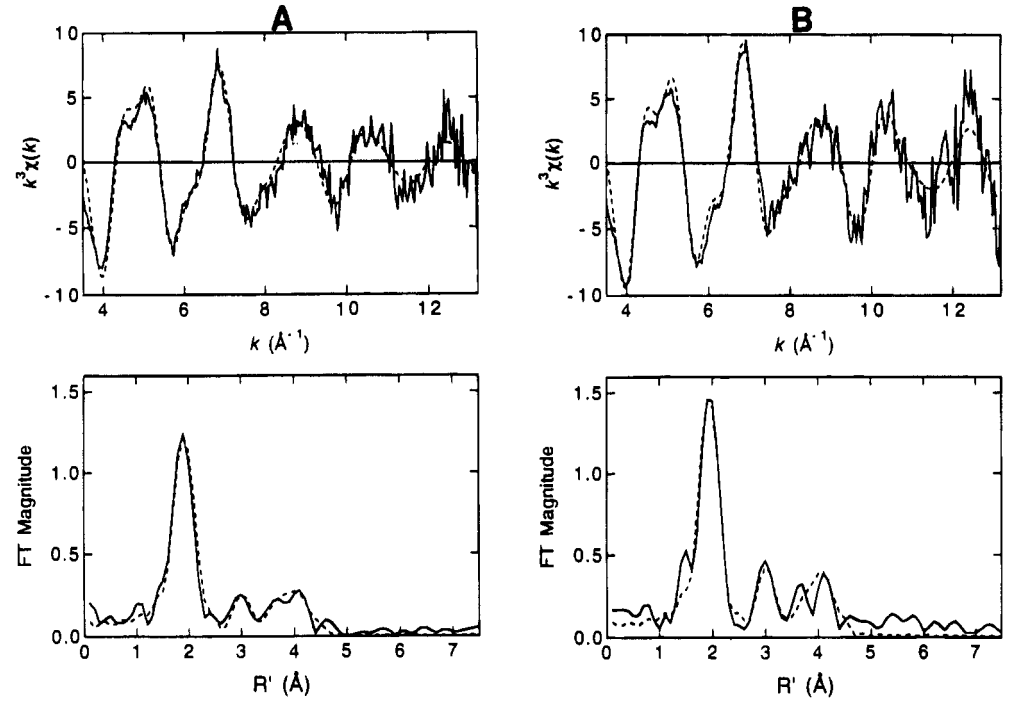

Figure 5. EXAFS (top) and Fourier transforms (bottom) of ferrocyanide-reduced and ferricyanide-oxidized galactose oxidase. (A) Reduced (inactive) galactose oxidase at pH 7.0. (B) Oxidized (active) galactose oxidase at pH 7.0. FTs were generated as in Figure 4. The fits from Table 2 are shown as dashed lines.

the original 1.7-Å crystal structure at pH 4.5. Given the reported differences in the crystal structures at pH 4.5 and 7.0, it is important to determine whether there are corresponding differences in the spectroscopic properties of the copper site. Galactose oxidase EPR spectra at pH 4.5 and 7.0 are compared in Figure 2. The EPR spectrum at 77 K and pH 7.0 is essentially identical to those reported previously.[2,3,7,10] At *both* pHs the g values and $A_{\parallel}$ values are typical of tetragonal Cu(II) complexes with N,O-donor ligands and hence consistent with the reported crystal structure at pH 4.5. The superhyperfine structure in the $g_{\perp}$ regions of both 77 K spectra is attributable to the coordinated imidazole nitrogens; other than being better resolved at pH 4.5, the superhyperfine structure is essentially identical at pH 4.5 and 7.0. On the basis of the EPR spectra, there are, at most, relatively minor structural variations between room temperature and 77 K at either pH 4.5 or 7.0.

Possible variations in the Cu(II) site as a function of pH or

(26) Scott, R. A.; Wang, S.; Eidsness, M. K.; Kriauciunas, A.; Frolik, C. A.; Chen, V. J. *Biochemistry* **1992**, *31*, 4596–4601.
(27) Wang, S.; Lee, M. H.; Hausinger, R. P.; Clark, P. A.; Wilcox, D. E.; Scott, R. A. *Inorg. Chem.* **1994**, *33*, 1589–1593.
(28) Scatchard, G. *Ann. N.Y. Acad. Sci.* **1949**, *51*, 660–665.
(29) This method for analyzing the data was derived by Dr. David Herries, University of Leeds.

Table 2. EXCURVE Curve-Fitting Results for Cu EXAFS of Galactose Oxidase[a]

sample	fit[b]	group	shell	N_s	R_{as} (Å)	σ_{as}^2 (Å^2)	f'[c]
GOase, as isolated, pH 7	4A	imid	Cu−N_1	(2)[d]	1.97	0.0035	0.067
		imid	Cu−C_2		2.93	0.0060	
		imid	Cu−N_3		4.10	0.0080	
		imid	Cu−C_4		4.15	0.0085	
		imid	Cu−C_5		3.01	0.0060	
			Cu−O	(2)	1.95	0.0060	
			Cu−S	(1)	3.42	0.0130	
GOase, as isolated, pH 4.5	4B	imid	Cu−N_1	(2)	1.97	0.0025	0.057
			Cu−C_2		2.93	0.0055	
		imid	Cu−N_3		4.10	0.0090	
		imid	Cu−C_4		4.15	0.0090	
		imid	Cu−C_5		2.99	0.0060	
			Cu−O	(2)	1.97	0.0060	
			Cu−S	(1)	3.45	0.0120	
GOase, $Fe(CN)_6^{4-}$-reduced	5A	imid	Cu−N_1	(2)	1.95	0.0035	0.063
		imid	Cu−C_2		2.91	0.0085	
		imid	Cu−N_3		4.08	0.0110	
		imid	Cu−C_4		4.13	0.0110	
		imid	Cu−C_5		2.98	0.0085	
			Cu−O	(2)	1.97	0.0080	
			Cu−S	(1)	3.47	0.0105	
GOase, $IrCl_6^{3-}$-oxidized	5B	imid	Cu−N_1	(2)	1.97	0.0020	0.053
		imid	Cu−C_2		2.93	0.0040	
		imid	Cu−N_3		4.10	0.0070	
		imid	Cu−C_4		4.15	0.0070	
		imid	Cu−C_5		2.99	0.0040	
			Cu−O	(2)	1.96	0.0075	
			Cu−S	(1)	3.47	0.0140	

[a] Group is the chemical unit defined for the multiple scattering calculation. N_s is the number of scatters (or groups) per metal; R_{as} is the metal-scatterer distance; σ_{as}^2 is a mean square deviation in R_{as}.[b] The fits are named according to the figures in which they are illustrated. [c] f' is a goodness-of-fit statistic normalized to the overall magnitude of the $k^3\chi(k)$ data:

$$f' = \frac{\{\sum[k^3(\chi_{obsd}(i) - \chi_{calc}(i))]^2/N\}^{1/2}}{(k^3\chi)_{max} - (k^3\chi)_{min}}$$

[d] Numbers in parentheses were not varied during optimization.

the redox state of the coordinated tyrosine were also assessed by XAS. All the XAS data were collected at low temperature (10 K) to minimize radiation damage to the samples. XAS data as a function of pH were collected on the resting (as isolated) enzyme in order to correspond as closely as possible to the galactose oxidase samples in the crystallographic work. Copper K-edges are shown in Figure 3A for reductively-inactivated and oxidatively-activated samples; the edges are similar and are consistent with a Cu(II) oxidation state in both samples, in agreement with previous results.[15] The minor shift in the lower portion of the edge may indicate a small fraction of Cu(I) in the ferrocyanide-reduced enzyme (Figure 3A). Shown in Figure 3B is a comparison of the edges obtained at pH 4.5 and 7.0 for the resting form, which are virtually identical and again consistent with Cu(II). We have observed that the copper K-edge is somewhat variable from one galactose oxidase sample to another, which perhaps reflects minor variations in composition. These minor variations in the edges are not correlated with significant variations in the EXAFS. EXAFS data are collected in Figures 4 and 5, and the fits are summarized in Table 2. The galactose oxidase EXAFS is very similar at the two pH values examined, with the possible exception of additional outer-shell scattering at pH 4.5 (note the increased intensity in the 3-Å FT peak in Figure 4B) that may be associated with the acetate ligand. The EXCURVE curve-fitting results of the galactose oxidase EXAFS are very satisfactory for all the samples examined (Table 2; Figures 4 and 5). Minor differences between data and simulation in the 3.5−4.0-Å region of the FT in Figure 5B result from apparent resolution of a 3.7-Å peak, which we believe is caused by the greater noise in the EXAFS of that sample. Overall, the EXAFS data for the Cu(II) forms (resting, reductively-inactivated, oxidatively-activated) of galactose oxidase at either pH 4.5 or 7.0 are consistent with the presence of two imidazole ligands and one or two additional first-shell ligands, modeled as Cu(II)−O. The outer-shell scattering features, evident at $R' = 3$ Å and $R' = 4$ Å in the Fourier transforms in Figures 4 and 5, are well modeled by two coordinated imidazoles. The bond distance of 1.95−1.97 Å (R_{as} in Table 2) is not unusual for equatorial Cu(II)−imidazole bonds; it agrees with the crystallographic distance[4,5] of 2.1 Å for His496 and His581, given the average positional errors in the X-ray structure (0.16 Å) and the possible ~0.1 Å *spread* of unresolved distances to a disordered first shell of scatterers from the EXAFS fits.[30] The equatorial Cu(II)−O distances from EXCURVE are practically identical to the Cu(II)−N distances (Table 2), but the Debye−Waller factors (σ_{as}^2) are larger, indicating some disorder. Since the positional error for the acetate ligand in the X-ray structure may be higher than the average,[5] the copper−oxygen distances derived from EXAFS and X-ray diffraction agree satisfactorily at pH 4.5, within the estimated experimental uncertainties. The EXAFS data suggest a more uniform set of bond distances within the equatorial plane than implied by the X-ray structures, although we emphasize that the actual differences at pH 4.5 between the crystal structure and the EXAFS fits are within the experimental uncertainties. No improvement in the EXAFS fit is obtained by including Tyr495, a result that is expected on the basis of the long 2.7-Å Cu−O distance. Our EXAFS data and fits are consistent with recent independent results.[31] Clark *et al.* reported a slight decrease in the average Cu−(N/O) bond length following redox activation (oxidation),[31] which is not apparent in our fits.

An additional feature of the EXAFS fits should be noted. Some improvement is evident if a heavy scatterer is included at 3.4−3.5 Å in *all* the samples examined (average reduction in f' ranged from 6 to 10%). This is very close to the crystallographic distance between the copper and the sulfur atom in the Tyr272−Cys228 thioether bond.[5] It is very difficult to detect even heavy scatterers at such a distance in the EXAFS, and a sulfur at 3.4−3.5 Å is not *required* to obtain an adequate fit, but it is interesting that such a feature consistently improves the fits. *Another key point established by the EXAFS results presented here is that there are no major structural differences between the reduced, inactive form of galactose oxidase and the oxidatively-activated form containing the tyrosine radical.* Importantly, this permits conclusions derived from spectroscopic studies of the paramagnetic [Cu(II)−tyr] state to be applied to the catalytically active [Cu(II)−tyr•] state, which is diamagnetic and therefore more difficult to probe.

The available spectroscopic data, including those reported here, are consistent with a tetragonal coordination geometry for Cu(II) at *both* pH 4.5 and 7.0, which is extremely well-precedented but in contrast with the crystallographic model at pH 7.0. Bond distances from the EXAFS fits are normal for Cu(II)−N,O complexes with square-pyramidal coordination. The crystallographic model at pH 7.0 currently has a Cu−N distance of 2.2 Å (His581 and His496) and a Cu−O distance of 1.9 Å for the equatorial tyrosine (Tyr272); the bond length for the axial Cu−O bond with Tyr495 is 2.6 Å, and the closest "equatorial" water molecule has a Cu−O distance of 2.8 Å.[5] Effectively the copper is nearly three-coordinate, since the 2.6-Å and 2.8-Å distances are too long for substantial bonding interactions. Moreover, scatterers at 2.6−2.8 Å would not

(30) Lee, P. A.; Citrin, P. H.; Eisenberger, P.; Kincaid, B. M. *Rev. Mod. Phys.* **1981**, *53*, 769−806.
(31) Clark, K.; Penner-Hahn, J. E.; Whittaker, M.; Whittaker, J. W. *Biochemistry* **1994**, *33*, 12553−12557.

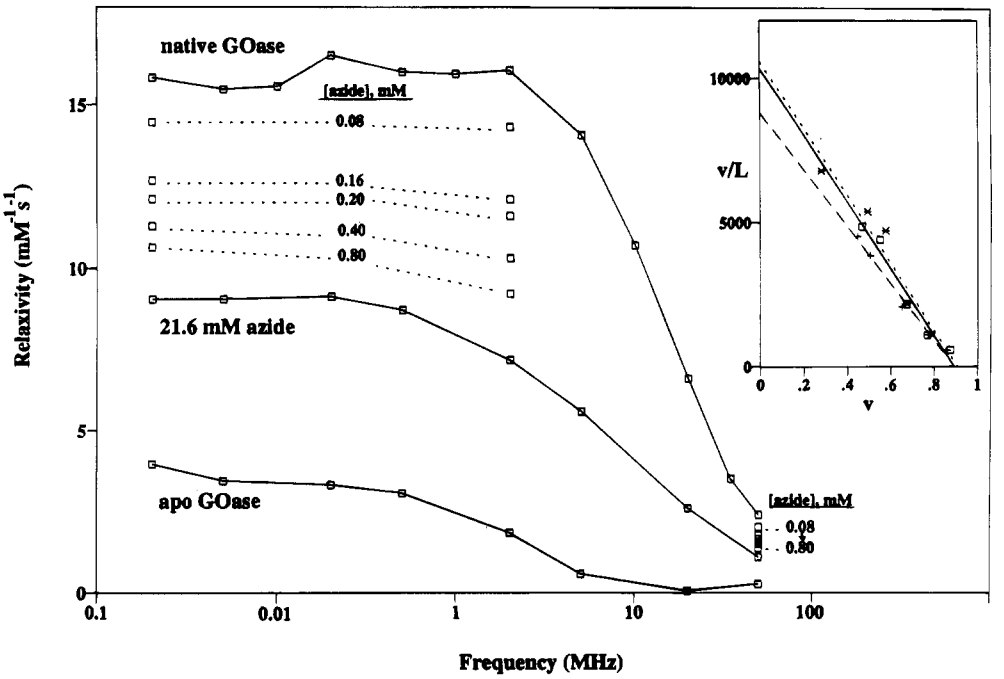

Figure 6. NMRD profiles of ferrocyanide-reduced galactose oxidase in the absence and presence of azide in 20 mM PIPES buffer, pH 7.0 at 298 K. The plots show the relaxivity ($1/T_1$, normalized for copper concentration) as a function of magnetic field, expressed as the proton Lamor frequency for a given field. The effects of adding azide on the relaxivity at field values corresponding to 0.02, 2, and 50 MHz are shown. No further decreases in $1/T_1$ were observed for azide concentrations in excess of 21.6 mM; the NMRD profile at this concentration is therefore taken to be that of the galactose oxidase–azide complex. The NMRD profile for apo galactose oxidase reflects the diamagnetic contributions to solvent proton relaxivity from the protein in solution. Inset: a Scatchard plot (concentration in M) of the changes in relaxivity at 0.02 MHz (□, —), 2 MHz (+, – –), and 50 MHz (×, - - -) accompanying the addition of azide. Data for each frequency were fit independently; the mean is $K = 10\,000 \pm 1000$ M^{-1}.

contribute significantly to the copper EXAFS, so the current crystallographic models would predict that the copper EXAFS at pH 7.0 would differ significantly from that at pH 4.5. Yet both the appearance of the EXAFS data and the quantitative fits are very similar at these pH values. Moreover, simulations using the crystallographic coordinates do not reproduce the observed EXAFS at pH 7.0. It should be noted that the galactose oxidase crystals at pH 7.0 were prepared by transfer of crystals from a pH 4.5 medium and then examined at room temperature. In contrast, XAS data were collected in frozen solutions at 10 K. Thus, as suggested previously,[31] these techniques may have examined different forms of the enzyme. Detailed spectroscopic studies of enzyme crystals are required to assess this possibility.

The structural models for the Cu(II) site in galactose oxidase derived from previous spectroscopic experiments[2,3,6–10,12,13] are in remarkable agreement with our results and the 1.7-Å crystal structure at pH 4.5. It is worth noting that spectroscopic and chemical modification experiments led to a model for the galactose oxidase active site that featured mixed tyrosine/histidine/water coordination with an overall square-pyramidal geometry for Cu(II).[2,3] A tryptophan residue was predicted to be within the active site, in close proximity to the copper ion.[32,33] More recently, the stacking of an aromatic residue with the active site radical was also predicted.[12] Certainly there are several novel active-site features that were not anticipated by the spectroscopic results, including the Tyr272–Cys228 thioether bond and the presence of both axial and equatorial tyrosine ligands, but overall the success of spectroscopy in elucidating active site properties of galactose oxidase has been remarkable.

NMRD Studies of Substrate Binding. We have probed the access of substrate and exogenous Cu(II) ligands to the galactose oxidase active site with NMRD measurements (Figures 6–8). Since the $1/T_1$ NMRD profiles provide direct information on

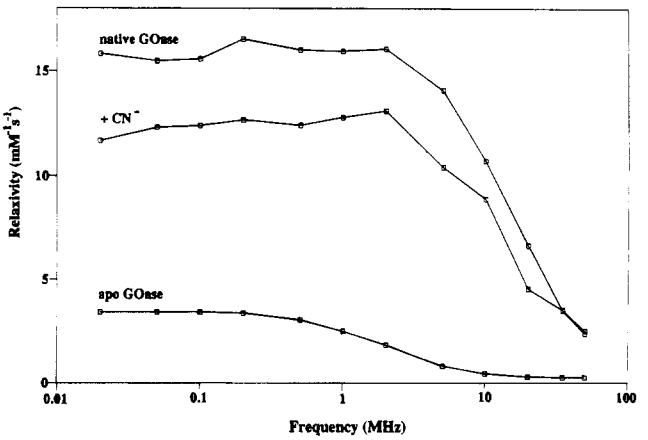

Figure 7. Effects of stoichiometric cyanide on the NMRD profile of ferrocyanide-reduced galactose oxidase in 20 mM PIPES buffer, pH 7.0 at 298 K. The plots show the relaxivity ($1/T_1$, normalized for copper concentration) as a function of magnetic field, expressed as the proton Lamor frequency for a given field.

the accessibility of paramagnetic sites, the reductively-inactivated [Cu(II)–tyr] form was used in these experiments. The NMRD profile of this form at pH 7.0, and the profiles of azide and cyanide complexes, are shown in Figures 6 and 7; Figure 8 shows the effects of adding the substrate dihydroxyacetone to the enzyme under anaerobic conditions. Since the experiments were conducted with inactive enzyme, no copper reduction by substrate should occur. Azide, cyanide, and substrate binding all cause significant decreases in the relaxivity $1/T_1$. Note that only stoichiometric cyanide was used, to minimize the possibility of copper reduction; it is likely that the galactose oxidase–cyanide complex is not fully formed

(32) Kosman, D. J.; Ettinger, M. J.; Bereman, R. D.; Giordano, R. S. *Biochemistry* **1977**, *16*, 1597–1601.

(33) Weiner, R. E.; Ettinger, M. J.; Kosman, D. J. *Biochemistry* **1981**, *16*, 1602–1606.

(34) Marwedel, B. J.; Kosman, D. J.; Bereman, R. D.; Kurland, R. J. *J. Am. Chem. Soc.* **1981**, *103*, 2842–2847.

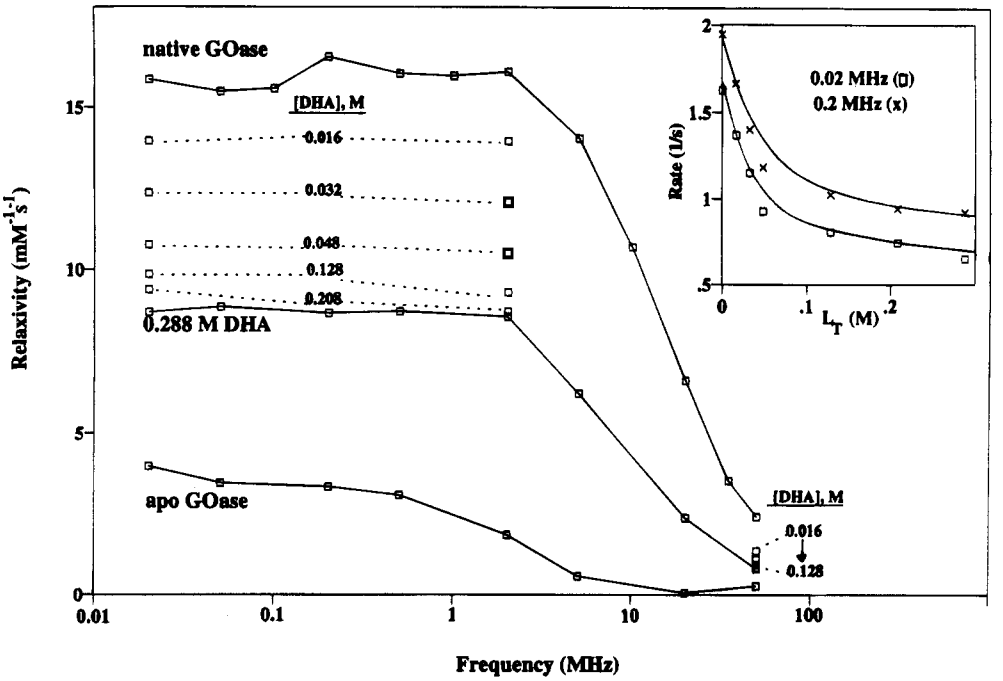

Figure 8. NMRD profiles of ferrocyanide-reduced galactose oxidase in 20 mM PIPES buffer, pH 7.0 and 298 K, in the absence and presence of dihydroxyacetone. The plots show the relaxivity ($1/T_1$, normalized for copper concentration) as a function of magnetic field, expressed as the proton Lamor frequency for a given field. The effects of adding the substrate dihydroxyacetone (DHA) at 0.02, 2, and 50 MHz are also shown. A complete profile at 0.288 M DHA was measured. Inset: Plot of the rate at 0.02 (□) and 2 (×) MHz as a function of the total concentration of DHA. Solid lines are the fits to eq 3 (see text).

under these conditions[34] and that further additions of cyanide would decrease $1/T_1$ to the level observed for the azide complex. Extensive spectroscopic studies have established that azide and cyanide coordinate to galactose oxidase Cu(II), almost certainly in an equatorial position. Recent X-ray crystallographic data confirm equatorial coordination by azide.[35] The NMRD results establish that these anions significantly perturb the relaxation of solvent H_2O protons by active-site Cu(II). An azide titration of galactose oxidase monitored by NMRD yielded a binding constant of 10^4 M^{-1} (Figure 6, inset), consistent with measurements using other techniques.[10] An analogous fit of substrate binding followed by NMRD changes gave a binding constant of 27 M^{-1} for dihydroxyacetone (Figure 8, inset), again consistent with previous estimates.[36] This strongly supports the conclusion that the observed decreases in $1/T_1$ are directly related either to exogenous ligand coordination to Cu(II) or to substrate binding to active site copper. Importantly, the NMRD profiles are very similar for the substrate and azide complexes, which is a strong indication that these species bind to the copper in the same way.

These conclusions are strengthened by the fact that the NMRD profile of galactose oxidase can be quantitatively accounted for by the rapid exchange of a single coordinated water molecule. A fit of the paramagnetic component ($1/T_{1P}$) of the NMRD profile to the Solomon equation, as modified by Bertini and co-workers to include electron–copper nuclear hyperfine coupling,[21,37] is displayed in Figure 9 and yields an average copper-proton distance of approximately 3 Å for a single coordinated water molecule. Assuming the standard geometry for water, the Cu(II)–O distance would be about 2.4 Å. The

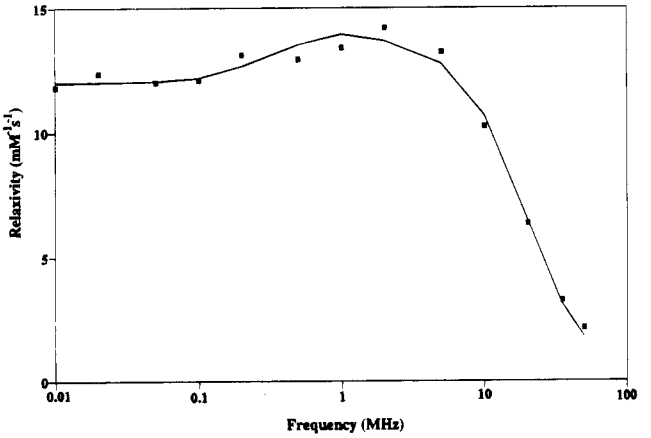

Figure 9. Paramagnetic contribution to the relaxivity ($1/T_{1P}$) and the fit to theory. ■ are the data normalized for copper concentration and with all diamagnetic contributions subtracted; the fit is shown as the solid line. The fit is that for a single water ligand at a distance of 2.4 Å in rapid exchange with solvent water. The following experimental values were used as input: $A_{||} = 186 \times 10^{-4}$ cm^{-1}; $A_{\perp} \simeq 0$; $g_{iso} = 2.129$. The electronic relaxation time of Cu(II) for the fit was calculated from the fit to be $\tau_s = 8.4 \times 10^{-9}$ s.

angle between the copper–proton vector and the z-axis of the copper nuclear hyperfine tensor for the fit shown in Figure 9 is 64°, which would place the coordinated water within or close to the equatorial plane. The quality of the fit establishes that the magnitude and shape of the NMRD profile are qualitatively and quantitatively consistent with a single, equatorial water ligand in fast exchange with bulk solvent with a Cu–O separation of about 2.4 Å (Figure 9). Both azide and cyanide, which are known to coordinate equatorially, significantly decrease the relaxivity by reducing the paramagnetic contribution $1/T_{1P}$, consistent with these ligands displacing the coordinated water molecule (Figures 6 and 7). Since binding of the substrate dihydroxyacetone produces analogous effects (Figure 8), the data strongly indicate that dihydroxyacetone also is coordinated equatorially.

(35) Ito, N.; Phillips, S. E. V.; Ogel, Z. B.; McPherson, M. J.; Keen, J. N.; Yadav, K. D. S.; Knowles, P. F. *Faraday Disc. Chem. Soc.* **1992**, *93*, 75–84.
(36) Zancan, G. T.; Amaral, D. *Biochim. Biophys. Acta* **1970**, *198*, 146–147.
(37) Bertini, I.; Briganti, F.; Luchinat, C.; Mancini, M.; Spina, G. *J. Magn. Reson.* **1985**, *63*, 41–55.
(38) Marwedel, B. J.; Kurland, R. J. *Biochim. Biophys. Acta* **1981**, *657*, 495–506.

Although the crystal packing prevents an analysis of substrate binding by X-ray diffraction, modeling studies also indicate that galactose, and presumably other substrates, coordinate *equatorially* to the Cu(II) in the galactose oxidase active site, in agreement with the NMRD results. A computer model for galactose coordination to copper is shown in Figure 1C.[5] The current model is in contrast to an earlier one, based on numerous spectroscopic experiments, which held that galactose would coordinate axially.[3] In part, the early spectroscopic model for substrate binding depends on the conclusion from $^{19}F^-$ NMR studies that water is a ligand at *both* axial and equatorial sites.[38] The X-ray structure establishes that Tyr495 is the only axial ligand. It is possible that high concentrations of fluoride, such as those used to detect the second binding site, displace the (weakly) coordinated axial tyrosine.[5] Another possibility is that the $^{19}F^-$ NMR-detectable fluoride does not coordinate to Cu(II) but rather hydrogen bonds to Arg330. The terminal NH_2 group of this residue is approximately 6.5 Å from the copper,[5] so Cu(II) should decrease the $^{19}F^-$ relaxation time (as observed). In addition, both acetate (at pH 4.5) and water (at pH 7.0) hydrogen bond to this residue in the crystal structures.[5] Direct NMR evidence for substrate coordination to Cu(II) is lacking. Attempts to monitor the binding of β-methylgalactose by ^{13}C NMR were not successful.[39] At the time, the absence of any detectable effect on the ^{13}C line width was rationalized in terms of axial binding.[39] This is not compelling evidence for axial coordination, particularly in light of the NMRD results and the highly complementary binding site for equatorial substrate coordination evident in the crystal structure.

In conclusion, our NMRD results are consistent with equatorial coordination by substrates as predicted by the crystal structure. NMR experiments to directly probe substrate binding with ^{13}C-labeled dihydroxyacetone may provide an alternative test of substrate coordination. The relaxivities of the azide and dihydroxyacetone complexes are about twice that of the apo protein and substantially larger than expected from outer-sphere relaxation.[40] This suggests that solvent water may bind weakly within the active site in the complexes, perhaps by hydrogen bonding to the coordinated ligand or Arg330. In fact the 1.7-Å map at pH 4.5 shows a moderately well-ordered water molecule H-bonded to Arg330, with a Cu–O separation of 4.7 Å. The NMRD data are further consistent with a single, rapidly exchanging water ligand with a Cu(II)–O(water) distance that is between the X-ray and EXAFS Cu–O distances. Clearly, more extensive spectroscopic and crystallographic experiments are warranted to address the questions raised by the galactose oxidase active-site structure at neutral pH. Our initial characterization of selected variants from site-directed mutagenesis indicates that this will be a fruitful approach.[41] Detailed ligand field and molecular orbital calculations, such as those carried out for the type 1 copper sites,[42] may also be helpful in correlating the structural possibilities and spectroscopic features of the galactose oxidase copper site.

Acknowledgment. We thank Nobutoshi Ito and Simon Phillips for numerous helpful discussions and Cynthia D. McCahon for excellent technical assistance. We are also grateful to Zicheng Xia and Claudio Luchinat for the fit of the NMRD data to theory and to Hui Zhang for help in the XAS data collection. XAS data were collected at the National Synchrotron Light Source (NSLS), Brookhaven National Laboratory, which is supported by the U.S. Department of Energy, Divisions of Materials Sciences and Chemical Sciences, and the Stanford Synchrotron Radiation Laboratory (SSRL), which is operated by the Department of Energy, Division of Chemical Sciences. The SSRL Biotechnology program is supported by the National Institutes of Health, Biomedical Resource Technology Program, Division of Research Resources. This research was supported by NIH Grants GM 27659 (D.M.D.) and GM 42025 (R.A.S.), a NATO Travel Award (D.M.D., P.F.K.), the SERC (P.F.K.), and the NSF Research Training Group Award to the Center for Metalloenzyme Studies at the University of Georgia (DIR 90-41281).

IC940994S

(39) Winkler, M. E.; Bereman, R. D.; Kurland, R. J. *J. Inorg. Biochem.* **1981**, *14*, 223–235.

(40) Koenig, S. H.; Brown, R. D., III. *Ann. N.Y. Acad. Sci.* **1973**, *222*, 752–763.

(41) Baron, A. J.; Stevens, C.; Wilmot, C.; Seneviratne, K. D.; Blakeley, V.; Dooley, D. M.; Phillips, S. E. V.; Knowles, P. F.; McPherson, M. J. *J. Biol. Chem.* **1994**, *269*, 25095–25105.

(42) Solomon, E. I.; Lowery, M. D.; LaCroix, L. B.; Root D. E. *Methods Enzymol.* **1993**, *226*, Part C, 1–33.